Controlling Laser Beam Speckle with Optimized Illumination of Zooming Phase Plates

Adeeb Sheikh

Advisor: Dr. Reuben Epstein
Laboratory for Laser Energetics, University of Rochester
Rochester, New York 14623-1299

1. ABSTRACT

Energy deposition by the laser during inertial confinement fusion implosion experiments [J. Nuckolls et al., *Nature (London)* 239, 139 (1972); S. Atzeni and J. Meyer-ter-Vehn, *The Physics of Inertial Fusion*, (Clarendon Press, Oxford, 2004).] is reduced by the shrinking surface area of the target with respect to the constant area of illumination of the laser. It has been proposed to reduce this energy loss by implementing a method called "two-state focal zooming," [D. H. Froula et al., Phys. Plasmas **20**, 082704 (2013).] wherein the illumination area of the laser is changed from a large initial area to a smaller area as the target implodes. The zooming is accomplished by utilizing a specialized distributed phase plate (DPP) [Y. Kato and K. Mima, *Appl. Phys. B* **29**, 186 (1982); Laboratory for Laser Energetics LLE Review 33, NTIS Document No. DOE/DP/40200-65, 1987 (unpublished), p. 1.] that has two sets of regions, each creating a different-sized focal spot where the beam is focused on-target. Different configurations of these "zooming phase plates" (ZPPs) produce speckle with unique spectra of spatial frequencies. To model these spectra, statistical models for discrete DPPs were generalized and implemented in a computer program that was applied to various ZPP configurations to find specific arrangements that reduce the speckle at lower spatial frequencies. Good agreement was obtained between the measured and predicted spectra for an experiment in which certain portions of a standard DPP were illuminated.

2. INTRODUCTION

Successful laser-driven fusion requires uniform target implosions. In order to accomplish this using the direct-drive method for inertial confinement fusion (ICF),[1] the spherical target must be uniformly irradiated. However, spatial aberrations in the wavefront of the laser cause intensity variations in the illumination incident on the target,[2] causing uneven energy deposition

and implosion asymmetry, and reduce the implosion performance. One method for smoothing the intensity profile of a laser beam is to utilize a distributed phase plate (DPP).[3]

DPPs are diffractive elements built with a varying thickness that breaks up the laser into spatially incoherent beamlets. The purpose is two-fold: to smooth the laser profile in the far-field by breaking the laser coherence and diminishing the effect of wave aberrations on illumination uniformity, and to increase the size of the focal spot in the far-field on-target to match that of the target. The superposition of each of these beamlets creates a fine-scale intensity pattern, or "speckle," that is much finer and smoother, relative to the original non-uniform intensity of the laser beam without the DPP. The speckle pattern arises because of the interference between the beamlets diffracted through the DPP. This speckle can be modeled as the product of an envelope function representing the smoothed beam shape and a modulation function, which adds "noise" to the envelope as a result of the random element in DPP diffraction and interference.

There are two types of DPPs: discrete and continuous. Discrete DPPs are constructed from a uniform honeycomb pattern of hexagonal area elements, with one of two different thicknesses, selected randomly, such that any one element will shift the phase of the light wave by 0 or π radians [Fig. 1].[3] In discrete DPP's, the light passing through each element is referred to here as a beamlet. Because of the random relative phase between the area elements of the DPP, the beamlets have properties of beams that propagate independently. The focal spots of all the beamlets are superimposed at the same focal spot on-target. Because of the diffractive properties of the discrete DPPs, energy is lost to the edges of the focal spot, coupling only 78% of the incoming energy onto the target. Thus, continuous DPPs replaced discrete DPPs. Their thickness varies continuously reducing the energy lost to the focal spot edge and increasing the energy focused onto the target to about 99%.[4] While the two types of DPPs are structurally different, they produce similar effects and have similar properties.[5] This would seem to allow the use of discrete DPP statistics in the context of modern continuous DPPs.

Two issues with the DPPs arise when considering the static size of the focal spot in the far-field. The first occurs because the target shrinks during implosion, causing light near the edge of the far-field to miss the target as implosion continues; naturally, this reduces the energy deposition onto the target. The second problem is a result of the first; errant light, which we visualize as rays, near the edge of the beam causes a phenomenon known as Cross-Beam Energy
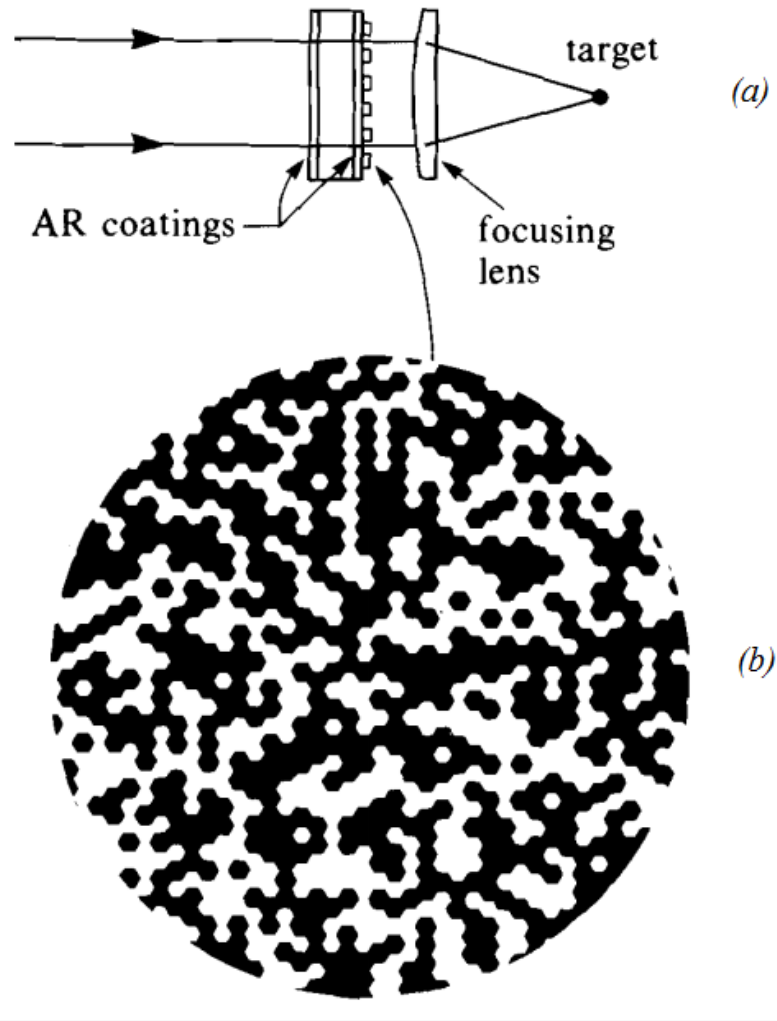
Fig. 1. (a) Principle of a distributed phase plate (DPP). The laser illumination that passes through each element of the DPP irradiates the whole target when focused by the lens. (b) A discrete DPP. This is binary in nature, with randomly distributed elements of two different thicknesses (shown as black and white) in order to evenly break the coherence of incoming laser light. [Figure from Ref. 3]

Transfer (CBET),[6] a multiple-beam laser-plasma interaction instability that further reduces the energy deposition of incoming light. CBET is a consequence of stimulated Brillouin scattering (SBS).[7] SBS occurs when intense laser light drives ion acoustic waves in a medium, causing the medium to act as a diffraction grating that scatters incoming light. CBET occurs when incoming laser light (the center-beam ray of Fig. 2) scatters into the outgoing off-center laser illumination

(the edge-beam ray of Fig. 2). This keeps much of the incoming light from reaching its innermost turning point where it would be most efficiently absorbed, thus reducing the energy deposition onto the target [Fig. 2].
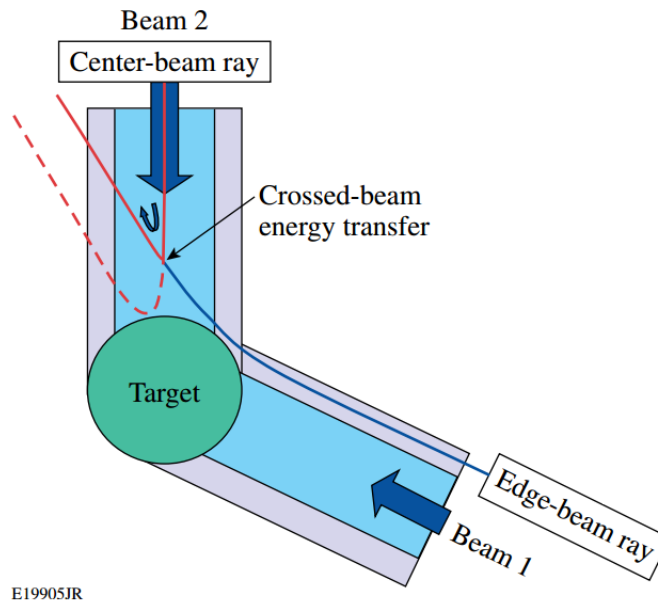

E19905JR

Fig. 2 Schematic of cross-beam energy transfer. Edge-beam rays miss the target completely and intersect the paths of incoming rays. The plasma-beam SBS interaction transfers incoming laser energy of the center-beam rays [such as the ray shown in red] to outgoing edge-beam rays [such as the solid blue ray], thus reducing the incoming energy that reaches the target surface. [Figure from Ref. 6]

3. TWO-STATE FOCAL ZOOMING

One proposed method for mitigating CBET involves dynamically changing the diameter of the focal spot of the laser in the far-field. This can be accomplished through a process known as two-state focal zooming,[8] wherein an initial picket pulse[9] is incident upon the target with a wide diameter focal spot, while the main pulse irradiates the target with a smaller focal spot. Two-state focal zooming has the benefit of mitigating CBET through a dynamic focal diameter, while still maintaining relative uniformity of implosion, by matching the illumination spot size to the target size, both early and late in the implosion.

The process itself involves illuminating specific parts of a specially designed DPP -- a Zooming Phase Plate (ZPP), such that the picket pulse will produce a wide diameter illumination
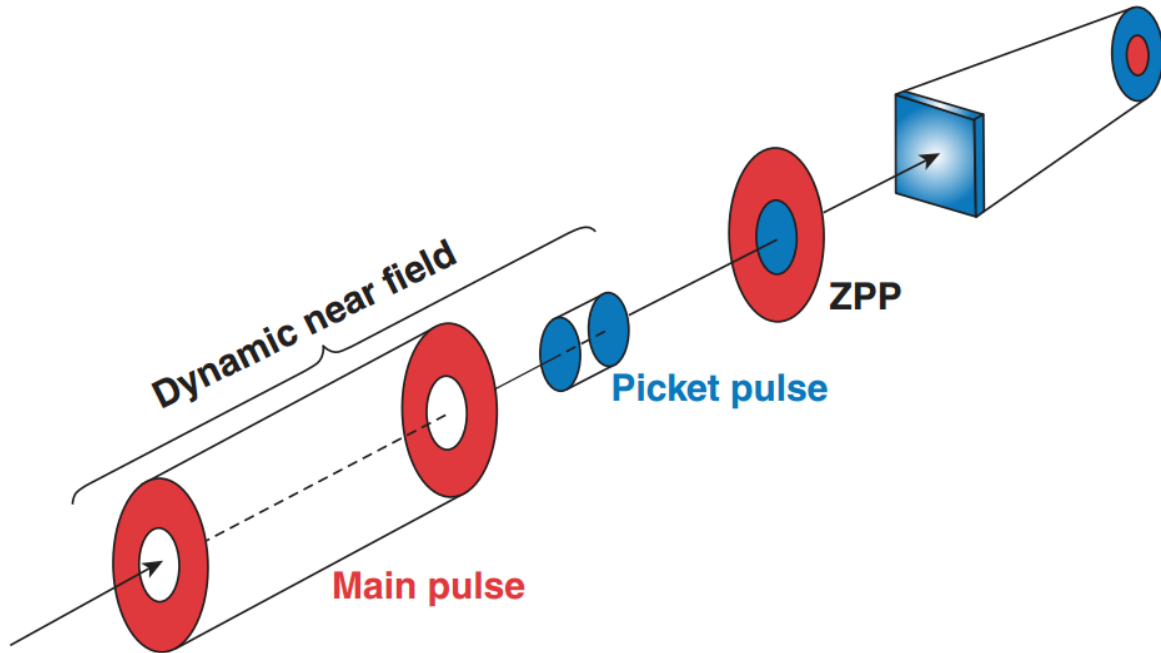
Fig. 3 Principle of a zooming phase plate (ZPP). The picket pulse is fired first, passing through a specific region of the ZPP with smaller "elements" (i.e. denser structure variations), creating a wide focal spot. Then the main pulse is fired through the rest of the ZPP with larger "elements," creating a focal spot with a reduced diameter. [Figure from Ref. 9]

in the far-field and the main pulse will produce a smaller diameter illumination [Fig. 3].[9] The ZPP functions because it consists of two types of regions: one which is illuminated by the picket pulse and one which is illuminated by the main pulse. The nature of these regions is such that their illumination yields different size focal spots. This is accomplished by exploiting the properties of DPPs. Consider a continuous DPP with shorter-scale or "dense" variations in thickness -- the equivalent of smaller elements in a discrete DPP. Illuminating this DPP, the focal spot would be larger than that of a continuous DPP with larger-scale or "sparse" variations in thickness. We can apply this principle to a ZPP by having regions of dense variations for the picket pulse and sparse variations for the main pulse [Fig. 4].[9] However, different ZPP designs produce different speckle spectra, depending on which regions of the ZPP are illuminated at any given time. To this end, it is necessary to identify an optimal configuration, where the most harmful spatial frequencies, the low frequencies, are minimized, in order to optimize the

5

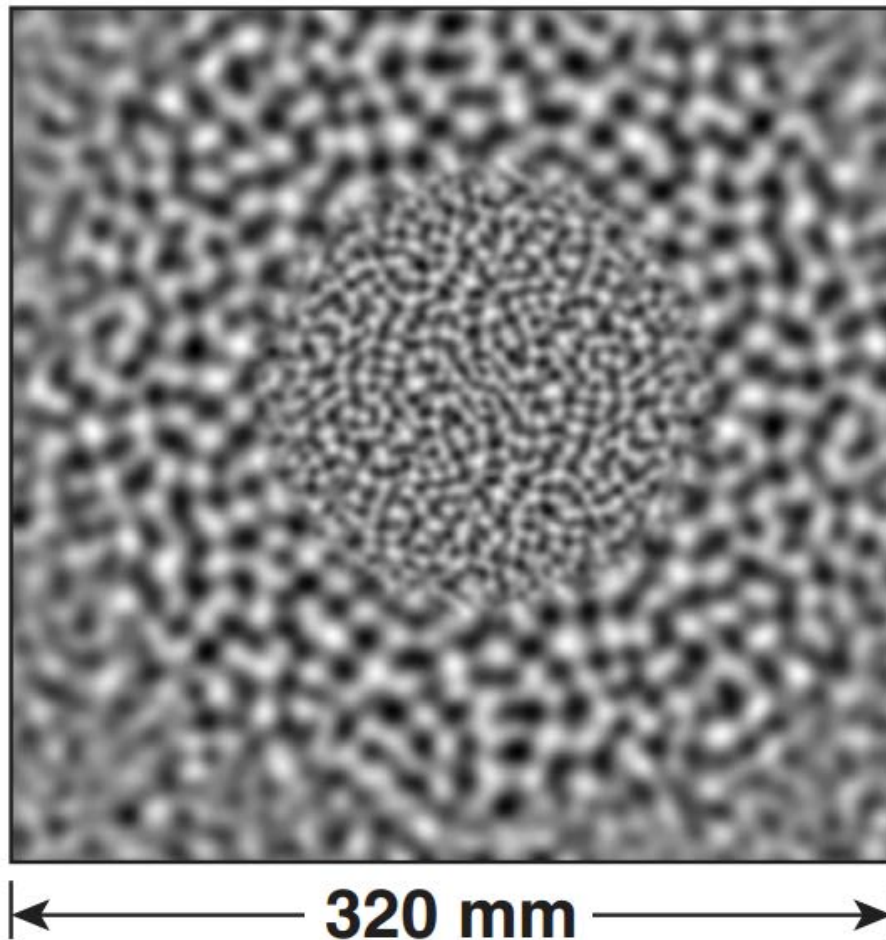uniformity of the energy deposition.

Fig. 4 A phase-contrast photograph of a continuous DPP with the phase contrast represented by shading. This is a ZPP, with a central and surrounding regions constructed with patterns characterized by different overall structure scale lengths selected for zooming from larger to smaller focal spots at the early and late stages of an implosion. [Figure provided by D. H. Froula]

4. DEVELOPING THE STATISTICAL MODEL AND SIMULATION

In order to determine the effectiveness of different ZPP configurations, it was first necessary to model the speckle spectrum and express it in terms of spectral density. This would show which spatial frequencies are most prominent in the far-field. Before developing such a model, however, it was important to lay down some assumptions: (1) the DPP in question is discrete, with a number of elements N, each of an area, a, resulting in a total illuminated area

$A=aN$; (2) the light is focused with focal length, z_0, wavelength, λ (or wave number, $k = 2\pi/\lambda$); and (3) the phase aberrations along the wavefront are negligible. The first assumption allows us to approximate the properties of continuous DPPs with those of discrete DPPs, which are much easier to calculate; the second assumption is simply a statement of the constants associated with the laser and optics; and the third assumption serves to simplify calculations, by avoiding the inherent problems of a real-world laser -- namely, the deformed wavefront.

The speckle of the intensity profile of the focused laser beams is expressed in our model as a modulation function. This modulation function represents the variations in the intensity of the laser projection on the target that arise because of the interference of beamlets after they have passed through the diffractive elements of a discrete DPP. The relationship between the intensity profile and the modulation function is expressed by

$$I(\vec{x}) = I_{env}(\vec{x})G(\vec{x}), \qquad (1)$$

where $I(\vec{x})$ represents the actual intensity profile of laser as a function of position on the target surface, $\vec{x}$, where $I_{env}(\vec{x})$ represents the smooth envelope of the intensity distribution, and $G(\vec{x})$ represents the modulation function [Fig. 5].[10] For the purposes of modeling speckle
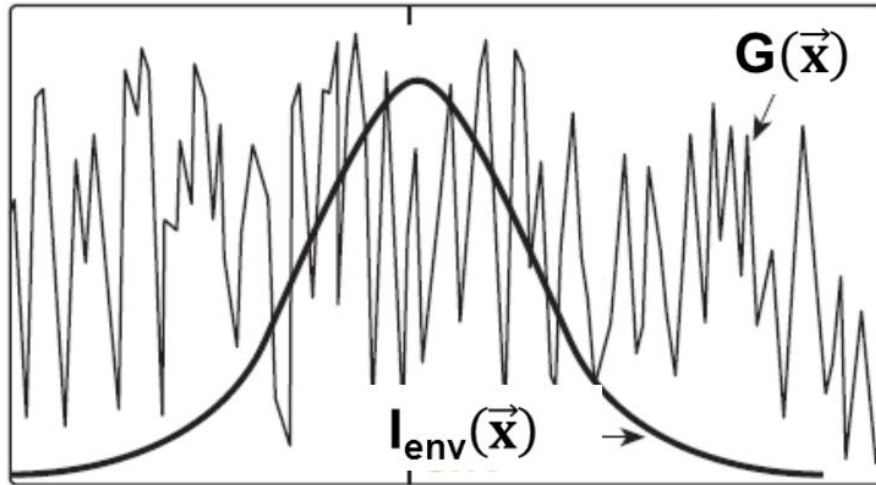

Fig. 5. A visual representation of the modulation function $G(\vec{x})$ and the intensity envelope $I_{env}(\vec{x})$ overlaid on the same set of axes. In expressing the intensity profile of a discrete DPP with Eq. (1), the envelope is the ideal smooth, "average" intensity profile that would be obtained with an individual beamlet, and the modulation function represents the speckle produced by the interference among all the superimposed beamlets. [Figure from Ref. 10]

spectra, the modulation function is expressed in terms of a phase correlation function $C(\vec{q})$, as

$$G(\vec{x}) = 1 + \sum_{\{\vec{q}\}} C(\vec{q}) e^{-i\vec{K}\cdot\vec{x}} \,, \tag{2}$$

such that the modulation function varies from unity by the sum of all products of the mean phase correlation function, $C(\vec{q})$, and the exponential of the dot product of the wave vector $\vec{K}$ and $\vec{x}$, summed over the set of all distinct element pair separations $\vec{q}$.[11] Each distinct $\vec{q}$ in the near-field plane corresponds to a spatial frequency component of frequency $\vec{K}$ in the far field. The specific relationship between $\vec{q}$ and $\vec{K}$ is

$$\vec{K} = \frac{k}{z_0} \vec{q} \,. \tag{3}$$

Because of the discrete nature of discrete phase plates, the DPP elements shift the phase of the incoming beamlets passing through element k at position $\vec{z}_k$ by $\phi(\vec{z}_k) = 0$ or π. Thus the phase difference between two elements will always be either 0 or π (modulo 2π) selected at random with equal probablilty. The mean phase difference between pairs of all illuminated phase plate elements of spatial separation $\vec{q}$ for a particular DPP is given by the spatial correlation function $C(\vec{q})$ expressed as the sum

$$C(\vec{q}) = \frac{1}{N} \sum_{k=1}^{N_{\vec{q}}} e^{i\left(\phi(\vec{z}_k + \vec{q}) - \phi(\vec{z}_k)\right)} \tag{4}$$

over all $N_{\vec{q}}$ illuminated element pairs with the spatial separation $\vec{q}$. In this expression, the exponentials of the phase differences, φ, between each two-element pair, k, with displacement $\vec{q}$ between them are summed and then divided by the total number of illuminated elements, N. The exponential expression, itself, equals -1 or 1 with equal probability. Formally, the mean value of $C(\vec{q})$ for each possible $\vec{q}$ and across all possible random phase differences, averaged over all possible different random DPP's, is 0, a result that is not helpful to our purposes. The typical value, however, is the square root of the mean square of $C(\vec{q})$ (or the "root mean square" or RMS). This value is non-zero and can be related to the area of intersection $A \cap A'$ between the

illumination area A and an exact copy of that illumination area A' displaced by the distance $\vec{q}$ as described in detail in Ref. 11, and expressed as

$$N^2 \left\langle \left| C(\vec{q}) \right|^2 \right\rangle = N_{\vec{q}} ,$$ (5)

where

$$aN_{\vec{q}} = A \cap A' \ .$$ (6)

Equation (5) is based on the statistics of the random walk where the length of a walk of n steps either forward or backward in a line, selected at random, is $\sqrt{n}$ steps, averaged over many walks. Just as no two random walks are identical, the speckle modulations of no two independently designed random DPP's are identical. Nevertheless, when they are constructed following the same rules, the same RMS statistical results apply to them all. The total RMS speckle modulation σ^2_{RMS} from any set of element separations $\{\vec{q}\}$ or, through Eq. (3), spatial frequencies $\{\vec{K}\}$ is the sum

$$\sigma^2_{RMS} = \sum_{\{\vec{q}\}} \left\langle C^2 (\vec{q}) \right\rangle.$$ (7)

In the limit of a DPP with a large number of small elements, this discrete sum can be expressed as an integral. The contribution to the total RMS speckle modulation by all $\vec{K}$ whose absolute values are within an infinitesimal interval dK of $K = (k/z_0)q$ is given by the spectral power density

$$\frac{d\sigma^2_{RMS}}{dK} = \frac{z_0}{k} \int_0^{2\pi} \left\langle C^2 (\vec{q}) \right\rangle \frac{q}{a} d\theta .$$ (8)

Using Eqs. (5) and (6) to substitute the area of intersection $A \cap A'$ for the mean square of the correlation function $C(\vec{q})$ in its relationship with spectral density of the speckle spectra, we obtain, continuing to follow the development in Ref. 11, the expression,

$$\frac{d\sigma^2_{RMS}}{dK} = \frac{z_0}{k} \int_0^{2\pi} \frac{(A \cap A')_{\vec{q}}}{A^2} q d\theta .$$ (9)

The integral over the angle θ in Eqs. (8) and (9) represents the sum over all $\vec{q}$ of the same length

to obtain the spectral power density with respect to the scalar separation $q = |\vec{q}|$ or the spatial frequency $K = |\vec{K}|$ for all directions.

While Eq. (9) contains in principle exactly what we need, there are some alterations to be made for our convenience. Namely, we want to express the spectral power density in terms of the normalized spatial frequency K / K_{max} and use the square root of the spectral power density given by Eq. (9) to express the amplitude of the spatial frequency terms of Eq. (2). Next, we must construct a discrete approximation of the integral appropriate for a numerical evaluation. Equation (9) provides the basis for developing the key algorithm of the computer program for the speckle simulation, henceforth referred to by its name: SPQL.

The first task in programming SPQL was to find the area of intersection between an arbitrary illumination area and that same illumination area displaced by $\vec{q}$. This was accomplished by representing the entire DPP surface with a square array of square array elements, each assigned the value with 1's and 0's as selected by a user, where a 1 or 0 indicates an illuminated or unilluminated area element of the DPP, respectively. These array elements are created as a discrete representation of an arbitrary illuminated area of the DPP surface; they are not to be confused with either the area elements of the phase-delay pattern of the DPP or their phase. The program then copies the illumination array and displaces it by $\vec{q}$. The number of intersecting illuminated area elements is then calculated by multiplying the assigned value of each element of the original illumination array by the value of the overlying element of the displaced illumination array, thus forming a product array, and then summing the values of all the numbers of this product array. The area of intersection is equal to the product of the number of intersecting area elements and the area of a single area element. This works because the only elements of the product array with a value of 1 are those where *both* factor array elements at the original and displaced position have a value of 1. These areas of intersection are then stored in a separate array, tabulated with respect to their associated displacements, so that it is possible to refer to them later and sum them as

$$\frac{d\sigma^2_{RMS}}{dK} = \sum_{(q-\Delta q/2 < |\vec{q}| < q+\Delta q/2)} \frac{\left(A \cap A'\right)_{\vec{q}}}{aN^2 \Delta q} \frac{z_0}{k}, \tag{10}$$

which is the discrete sum, corresponding to Eq. (9), forming the spectral power density of the

speckle, where Δq represents the element interval of the spacing of the discrete representation of the speckle spectrum or, through Eq. (3), the spatial frequency interval ΔK. Once we have tabulated the spectral power density function, we can obtain

$$\sqrt{\frac{d\sigma^2_{RMS}}{d\frac{K}{K_{max}}}} = \sqrt{\frac{\displaystyle\sum_{(q-\Delta q/2 < |\bar{q}| < q+\Delta q/2)} \frac{(A \cap A')_{\bar{q}}}{aN^2 \Delta q} \frac{z_0}{k}}{\frac{k}{z_0} q_{max}}} \, , \qquad (11)$$

the RMS amplitude spectrum of the DPP model speckle spectrum.

5. EVALUATING THE ACCURACY OF THE SIMULATION

It has been noted before that the simulation and corresponding model were developed specifically with the statistics of the discrete DPPs in mind. However, modern lasers such as OMEGA and the NIF use continuous DPPs. Thus, testing the accuracy of the discrete DPP simulation by comparing its results with continuous DPP laboratory measurements is especially important. Similarities between the two sets of results support the notion of the general similarity between discrete and continuous DPPs.[5]

We compared the modeled modulation spectrum with the measured modulation spectrum obtained by Mr. Terrence Kessler and Dr. Hu Huang for a ZPP configuration they selected.[12] The configuration they proposed involved the illumination of twelve circular areas distributed along a square lattice within the full circular aperture [Fig. 6(a)]. Visually, the modeled and measured amplitude spectra matched very well over all but the first small peak at the low end of the spatial frequency spectrum [Fig. 6(b)]. The spectral effects of the focal spot envelope and perhaps other characteristics unique to continuous DPP's are present in the measured spectrum at the low end. The modeled spectrum is of the speckle modulation function alone, while the speckle and the envelope of the measured spatial-frequency spectrum cannot be separated in a similarly well-defined way.

Nevertheless, for our purposes, a matched-pair t-distribution hypothesis test and the associated confidence intervals effectively demonstrate the model's predictive powers. The conditions for applying this test are met: the sample is random, as previously mentioned; the

11
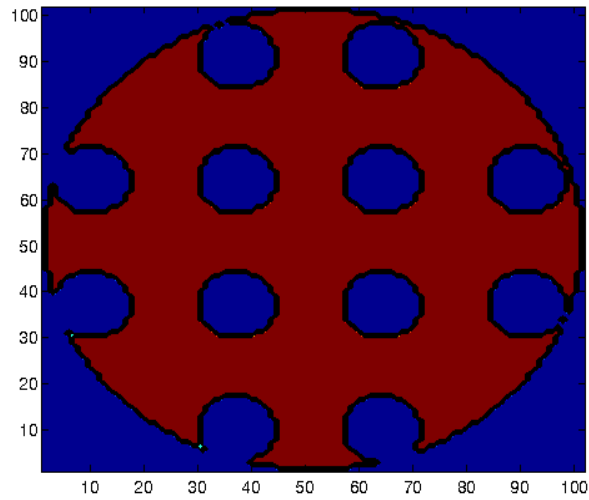
(a)
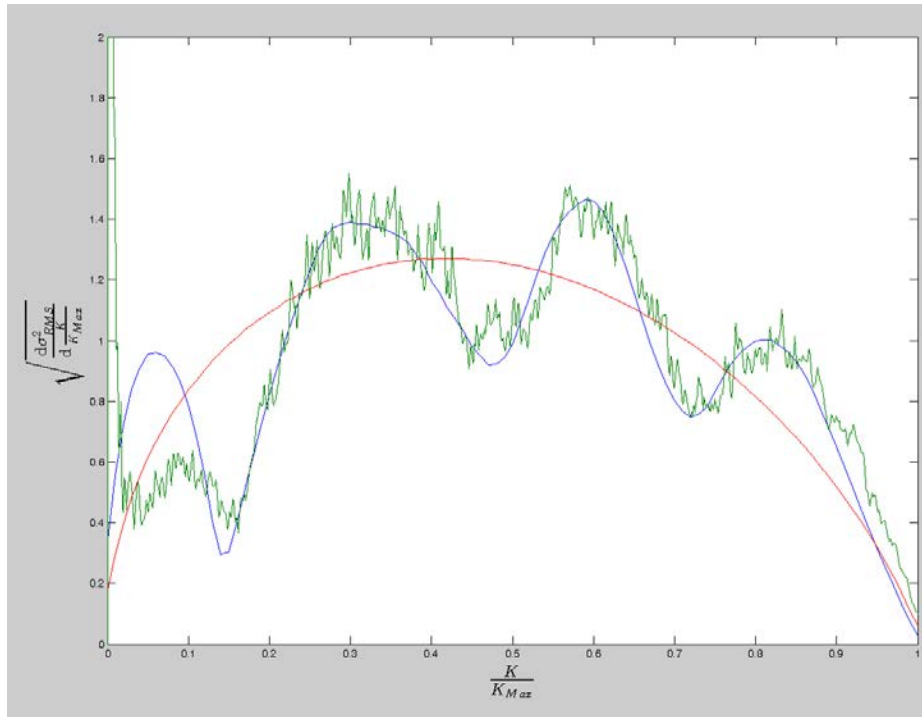
(b)

Fig. 6. (a) The 12-circle configuration of the ZPP. (b) The corresponding modeled amplitude spectrum in blue, the measured power spectrum in green, and the full-aperture power spectrum in red for comparison.

standard deviations of the error are unknown; internal independence is assured, as points in either the data set or the model are individually calculated and do not interfere with each other; the model and the data set are dependent, because they vary non-randomly and operate off a similar set of principles; and a sample size of 100 data points is large enough to assume a

normal-like distribution of the mean difference values.

The null hypothesis for the test is that the difference between the model and the data is zero, or insignificant; naturally, the alternative hypothesis is that they are not equal. The calculated sample mean difference and associated sample standard deviation are 0.01694 and 0.1788 respectively. From this we attain a P-value of 0.9247 for a t-distribution of sample size 100, which allows us to fail to reject the null hypothesis at a significance level of 0.05. Based on this test, we can say with 95% confidence that the true mean difference lies between -0.03378 and 0.03717. Performing similar operations for the mean percent difference, we calculated the sample mean percent difference, 2.928; the sample standard deviation, 24.71; the P-value, 0.2411; and a 95% confidence interval for the true mean percent difference between -1.999 and 7.856. Once again, we fail to reject the null hypothesis. Thus, there is significant evidence indicating that the model suitably predicts the behavior of continuous DPPs.

6. OPTIMIZING THE CONFIGURATION

With the verified model, it is possible to move towards the ultimate goal: optimizing ZPP configurations to reduce harmful spatial frequencies. Initial attempts consisted of simple trial-and-error designs, with new configurations based on intuition and basic calculations. Generally, we looked for configurations where elements of picket illumination are as far apart as possible, because if the q's between elements are generally made larger, the smaller, most harmful K frequencies are present to a reduced degree. Beyond that, there were no other criteria. Next, we implemented a different method of optimization known as "simulated annealing."[13] The idea behind the method is to make a small change to the configuration, then evaluate the resulting change in the power spectrum, and then decide whether or not to keep or reject the change. A subtlety of this standard method is that there is an adjustable probability, rather than a certainty, that favorable changes are accepted and unfavorable changes are rejected. This process is iterated many hundreds of times. The purpose of having a probability, rather than a certainty, of keeping or rejecting favorable or unfavorable changes, respectively, is to allow the annealing process to escape from so-called " local peaks" -- where harmful frequencies are minimized with respect to any immediate small change, but where continuing the search slightly further afield would find a more favorable minimization of the harmful frequencies.

Although the results of this calculation were very preliminary, we did learn something interesting and not altogether surprising: the most ideal configurations tended to have the picket pulse illuminate small, circular, radially distributed areas. More investigation is necessary, but this at least provides a starting point.

7. CONCLUSION

The discrete DPP models appear to satisfactorily predict the behavior of continuous DPPs used on OMEGA and the NIF. This can be particularly helpful in the study of two-state focal zooming and the search for an optimal picket pulse illumination. By distributing the illumination in an optimum fashion, harmful spatial frequencies can be reduced, and the energy lost due to CBET as a result of plasma perturbations can be minimized. The optimization process itself can be automated through "simulated annealing," which has already shown favorable preliminary results, even if the idea has not been thoroughly developed. Ultimately, this leaves another avenue of exploration for increased energy deposition -- a necessary development to achieve ignition.

8. ACKNOWLEDGEMENTS

REFERENCES

1. J. Nuckolls, L. Wood, A. Theissen, and G. Zimmerman, *Nature (London)* 239, 139 (1972); S. Atzeni and J. Meyer-ter-Vehn, *The Physics of Inertial Fusion*, (Clarendon Press, Oxford, 2004).

2. Y. Kato and K. Mima, *Appl. Phys. B* **29**, 186 (1982).

3. Laboratory for Laser Energetics LLE Review 33, NTIS Document No. DOE/DP/40200-65, 1987 (unpublished), p. 1.

4. Laboratory for Laser Energetics LLE Review 63, NTIS Document No. DOE/SF/19460-91, 1995 (unpublished), p. 126.

5. J. Kandlikar, 1999 Summer Research Program for High School Juniors at the University of Rochester's Laboratory for Laser Energetics—Student Research Reports, 1996 (unpublished).

6. I. V. Igumenshchev et al. Phys. Plasmas **19**, 056314 (2012); C. J. Randall, J. R. Albritton, and J. J. Thompson, Phys. Fluids **24**, 1474 (1981).

7. I. V. Igumenshchev, D. H. Edgell, V. N. Goncharov, J. A. Delettrez, A. V. Maximov, J. F. Myatt, W. Seka, A. Shvydky, S. Skupsky, and C. Stoeckl, Phys. Plasmas **17**, 122708 (2010); W. L. Kruer, *The Physics of Laser Plasma Interactions* (Addison-Wesley, Redwood City, CA, 1988).

8. I. V. Igumenshchev et al. Phys. Rev. Lett. **110**, 145001 (2013).

9. D. H. Froula, T. J. Kessler, I. V. Igumenshchev, R. Betti, V. N. Goncharov, H. Huang, S. X. Hu, E. Hill, J. H. Kelly, D. D. Meyerhofer, A. Shvydky, and J. D. Zuegel, Phys. Plasmas **20**, 082704 (2013).

10. Y. Kato, K. Mima, N. Miyanaga, S. Arinaga, Y. Kitagawa, M. Nakatsuka, and C. Yamanaka, *Phys. Rev. Lett.* **53**, 1057 (1984).

11. R. Epstein, J. Appl. Phys. **82**, 2123-2139 (1997).

12. T. Kessler and H. Huang, private communication.

13. W. H. Press <u>et al.</u>, *Numerical Recipes*, (Cambridge University Press, Cambridge, 1986), §10.9.